교육학석사학위논문

Real-time Fluorescence-Raman (Dual Modal) Endomicroscopic Imaging System for Multiplexed Diagnosis

다중 진단을 위한 실시간 형광-라만 내시경형 영상 시스템에 관한 연구

2012 년 8 월

서울대학교 대학원

과학교육과 화학전공

정 신 영

Real-time Fluorescence-Raman (Dual Modal) Endomicroscopic Imaging System for Multiplexed Diagnosis

지도교수 정 대 홍

이 논문을 교육학석사 학위논문으로 제출함

2012 년 8 월

서울대학교 대학원

과학교육과 화학전공

정 신 영

정신영의 교육학석사 학위논문을 인준함

2012 년 8 월

위 원 장 _____ 유 재 훈 _____ (인)

부위원장 _____ 정 대 홍 _____ (인)

위 원 _____ 노 태 희 _____ (인)

Abstract

Real-time Fluorescence-Raman (Dual modal) Endomicroscopic Imaging System for Multiplexed Diagnosis

Sinyoung Jeong
Department of Science Education
(Major in Chemistry)
The Graduate School
Seoul National University

Recently, sensitive optical bio-imaging techniques have been developed for pre-diagnostics of disease, therapeutic application, and monitoring of disease progression in living animal using fluorescence dye, quantum dot, single walled carbon nanotube and noble metal nanoparticle (NP). Especially, by utilizing Surface Enhanced Raman Scattering (SERS) effect noble metal NP can provide high

sensitivity and high multiplexing capability, which are requested for *in vivo* multiplex bio-imaging. The SERS signal has significant advantages for multiplexed detection: A narrow spectral band of less than 1 nm, photo-stability with non-bleaching feature, and flexible selectivity of photo-excitation source. Owing to these advantages, SERS active nanoprobes can be used for multiplexed imaging of numerous bio-targets on tissues or organs. Several groups have reported that specific advantages of fluorescence, quantum dots, and Raman spectroscopy can be combined, in order to get additional functionality in *in vivo* multiplex bio-imaging.

In this study, we designed the real-time fluorescence-Raman (dual modal) endomicroscopic imaging system (FREIS) for multiplexed diagnosis with fluorescence-SERS active nanoprobes (F-SERS dots) based on fiber-optic light collection and two-dimensional laser scanning system. FREIS can simultaneously detect the fluorescence and SERS signal taking advantages of intense signal of fluorescence and multiplex capacity of Raman scattering. For this purpose, FREIS was designed to consist of three components: i) Dual-axis laser scanning unit, ii) a separation unit of fluorescence and Raman signals, iii) light detection unit with a photodiode for fluorescence signal and a spectrometer equipped with a CCD detector for SERS signal. The synthesized fluorescence-SERS active dots (F-SERS dots) were composed of silver NP assembles on silica backbone, and silica shell doped with rhodamine B isothiocyanate (RITC) and silver NPs were labeled with three kinds of Raman compounds for multiplexing: Rhodamine B isothiocyanate

(RITC), fluorescein isothiocyanate (FITC), and 4-aminothiophenol (4-ABT). Fluorescence and SERS signal are successfully separated each other by two optical filters. The fluorescence is utilized for imaging the targeted positions by F-SERS dots, and SERS signal is utilized to distinguish the kinds of three different F-SERS dots. Combining with F-SERS dots, FREIS can provide real-time fluorescence images (12 images/s). Since this imaging system is based on the optical fiber bundle, it has significant advantage like fiber optics-based endomicroscopy. However, optical fiber bundle gives a strong intrinsic Raman scattering background by optical fiber itself, which increases optical noises and reduces the spectral window for Raman spectroscopy. To circumvent this problem, a spectral window with less background noises was selected and fluorescence dye and Raman reporter molecules were chosen to fit in the selected spectral window. As a proof-of-concept experiment, various concentration of the F-SERS dots were measured on the slide glass and the phantom tissues using FREIS. These results exhibit that the developed imaging method comprised of the optical system and F-SERS probes can be applied to real-time *in vivo* multiplex bio-imaging.

Key words: Fluorescence, Surface Enhanced Raman Scattering (SERS), Real-time Multiplex bio-imaging, Fluorescence-Raman Endomicroscopic Imaging System (FREIS)

Student number: 2010-21534

Contents

List of Figure

1. Introduction

In recent years, sensitive optical bio-imaging techniques have been developed with an overwhelming interest for pre-diagnosis of disease, therapeutic application, and monitoring of disease progression in living animal; for this optical bio-imaging, sensitive optical nanoprobes and imaging systems are required.[1-6] Furthermore, because multiple biomarkers are expressed for a specific disease,[7] simultaneous multiplex detection methods are also required for highly accurate diagnosis of disease. In these regards, many researchers have tried to develop the highly sensitive and multiplex optical bio-imaging systems using near-infrared (NIR) fluorescence, inorganic metal nanocrystals (called as quantum dots, QDs), and noble metal nanoparticle (NPs).[8-10]

NIR fluorescence dye has been widely used for *in vivo* bio-imaging with low autofluorescence of biomolecules. However, it has several limitations for multiplex *in vivo* bio-imaging such as a large spectral overlapping and photobleaching.[11,12] Semiconductor QDs have emerged.[13,14] Despite quantum dots have significant advantages such as brighter fluorescence and less-photobeaching, it have cytotoxicity for living animal *in vivo* bio-imaging.[15] In addition, QDs have still broad spectral emission bands, which can limit their multiplex capabilities. Noble metal NPs have been used for bio-imaging due to their unique optical properties involving generation of strong localized surface plasmon (LSP). When a molecule is adsorbed onto the roughened surface of noble metal nanostructure, the molecule

experiences a drastic amplified incident electromagnetic field due to the LSP of noble metal structure.[16] Raman signal from the molecules on the surface of noble metal structure was drastically enhanced. This phenomenon has been known as surface enhanced Raman scattering (SERS). As a result, SERS signal is 10-14 orders of magnitude higher than normal Raman signal, providing the sensitivity required for optical in vivo bio-imaging. SERS has significant advantages for multiplexing detection: a narrow spectral band, photo-stability, and flexibility selectivity of photo-excitation source.[17-19] Therefore, SERS active nanoprobes can be used for multiplexed imaging of numerous bio-targets on tissues or organs. Moreover, several groups have been reported that the SERS active nanoparticles were combined with fluorescence dye or QDs in order to overcome obstacle of *in vivo* multiplex bio-imaging.[8,9,20,21]

Thus far, several optical imaging techniques have been applied to detect biomolecules in living animals. However, in the *in vivo* optical imaging, the limitation of penetration depth of light source has remained as a significant difficulty. Several optical bio-imaging systems based on the optical fiber have been developed as an alternative for living object *in vivo* imaging.[16,21-27] Especially, fiber optic-based endomicroscopy has significant potential for *in vivo* bio-imaging because it is possible to bring the fiber optics to proximity of tissues of interest, even inside the body organ, without the low depth of penetration issues. Furthermore, fiber optic-

based endomicroscopy enable to minimally invasive procedure to identify multiple biomolecules *in vivo* detection of living object.

In this study, we introduce that developed real-time fluorescence-Raman endomicroscopic imaging system (FREIS) for multiplexed diagnosis using fluorescence-SERS nanoprobes (F-SERS dots) to overcome these obstacles for bio-imaging; it can detect the fluorescence and SERS signal simultaneously. In this regard, we synthesized the F-SERS dots which could emit the fluorescence and SERS signal at the same time, and these probes were measured by optical fiber bundle of FREIS in order to evaluate the capability of this system; actually the fluorescence signal was utilized to imaging for tracking the targeted F-SERS probes, and the SERS signal was utilized to identify the kinds of F-SERS probes. After that, to demonstrate *in vivo* and *in situ* detection, we investigated the F-SERS dots on the slide glass and the surface of phantom tissue, at the various concentration of them.

2. Experimental Section

2.1 Chemicals and materials

Tetraethylorthosilicate (TEOS), 3-mercaptopropyl trimethoxysilane (MPTS), ethylene glycol (EG), silver nitrate ($AgNO_3$, 99.99+ %), 3-aminopropyltriethoxy-silane (APS), octylamine (OA), rhodamine B isothiocyanate (RITC), fluorescein isothiocyanate (FITC), and 4-aminothiophenol (4-ABT) were purchased from Sigma-Aldrich Inc. and used without further purification. Absolute ethanol (99.9 %), ammonium hydroxide (NH_4OH, 27 %), 2-propanol (99 %) and ethanol (98 %) were purchased from Daejung (Busan, Korea). Deionized (DI) water was used for all experiments.

2.2 Preparation of fluorescence surface-enhanced Raman scattering probes (F-SERS dots)

The *ca.* 120 nm sized Silica nanoparticles (NPs) were synthesised by the Stöber method.[28] Tetraethylorthosilicate (TEOS, 1.6 mL) was dissolved in 40 mL of absolute ethanol. After that, ammonium hydroxide (3 mL) was added into the solution. The resulting mixture was vigorously stirred using magnetic bar for 20 h at 25 ^{o}C. The silica NPs were centrifuged and then washed with ethanol several times to remove the excess reagents. These silica NPs were then functionalized with thiol group. The silica NPs (100 mg) were dispersed in 2 mL ethanol containing 100 μL of MPTS and 20 μL of ammonium hydroxide. The mixture was stirred for 2 h at 25

^{o}C. After that, the resulting thiol-functionalized silica NPs were centrifuged and washed with ethanol several times. A 100 mg of thiol-functionalized silica NPs was thoroughly dispersed in 50 mL of 0.03 mM $AgNO_3$ solution in ethylene glycol. An 82.7 μL of octylamine was then rapidly added into the thiol-functionalized silica NPs dispersed $AgNO_3$ solution in ethylene glycol. The resulting dispersion was stirred for 1 h at 25 ^{o}C. Afterwards, the silver embedded silica NPs (Ag silica) were centrifuged and washed with ethanol several times for purification. These Ag silica were labeled by three different kinds of Raman compound: RITC, FITC, and 4-ABT. A 10 mg of Ag silica were dispersed in containing each Raman compound solution in 1 mL ethanol: 1 mM of RITC, 1mM of FITC, and 100 mM of 4-ABT. The dispersion was shaken for 30 min at 25 ^{o}C. The Raman labeled Ag silica were centrifuged and washed with ethanol two times to remove excess reagents. These Raman labeled Ag silica were coated by silica shell in order to prevent aggregation and fluorescence quenching. A 10 mg of Raman labeled Ag silica were dispersed in 24 mL of mixed solution of 2-propanol (20 mL) and D.I water (4 mL). A 200 μL of ammonium hydroxide was then added into this dispersion. A 5 μL of TEOS was added into the mixed dispersion two times with interval of 2 h and then stirred for 6 h. The silica coated Raman labeled Ag silica were centrifuged and washed with ethanol several times for purification. In the next step, these Raman labeled Ag silica were encapsulated by a fluorescence dye conjugated silica shell. A 50 μL of 19.2 mM 3-aminopropyltri-ethoxysilane (APS) in ethanol and 5 μL of 8 mM RITC were

mixed for conjugation of APS and fluorescence dye (RITC). The resulting solution was stirred for 15 h at 25 ^{o}C. A 10 mg portion of silica coated Raman labeled Ag silica was dispersed in 24 mL of mixed solution of 2-propanol (20 mL) and D.I water (4mL). A 55 μL of RITC-APS conjugated solution was added into this dispersion. After that, a 10 μL of TEOS and 0.5 mL of NH_4OH were added into this dispersion. This dispersion was stirred for 9 h at 25 ^{o}C. The synthesized F-SERS dots were centrifuged and washed with ethanol several times for purification.

2.3 Instruments

Raman measurements were performed using a confocal microscope Raman system (LabRam 300, JY-Horiba, France) equipped with an optical microscope (BX41, Olympus, Japan). In this system, the Raman scattering signals were collected in a back-scattering geometry and detected by a spectrometer equipped with a thermo-electrically cooled (-70 ^{o}C) CCD detector. The spectrometer was equipped with two diffraction gratings: 300 grooves/mm and 1800 grooves/mm. The excitation source was diode-pumped solid-state 532 nm laser (CL532-100-S, Crystal, USA). Focusing of excitation laser and collection of Raman signal were done by same objective lens of x100 (NA 0.90, Olympus, Japan). The strong Rayleigh scattered light was eliminated by long-pass edge filter. The SERS spectra were taken with laser power of 4.3 mW, acquisition time of 1 s, and diffraction grating of 1800 grooves/mm. The fluorescence spectra were taken with laser power of 0.3 mW, acquisition times of 10 s, and diffraction grating of 300 grooves/mm. The laser power was controlled by inner neutral density filter (N.D. filter).

Real-time fluorescence-Raman endomicroscopic imaging system (FREIS) was used the fiber-coupled continuous wave diode-pumped solid-state 532 nm laser (Cobolt Samba^{TM}, Cobolt, Sweden) with 300 mW as an excitation source. The dual-axis laser scanning unit (Cell-Vizio^{TM}, Mauna Kea Technologies, France) was used for real-time scanning of the detecting area using optical fiber bundle. The spectrometer (SR 303i-A, Andor Tech., UK) with a thermo-electrically cooled (-50

^{o}C) detector CCD (DV401A-BV, Andor Tech., UK) was used for Raman detection. The separation unit was used two kinds of optical filters: dichroic filter (FF593-Di03-25D, Semrock Inc., USA) and long-pass filter (LP03-532RS-25, Semrock Inc., USA). Real-time FREIS was composed of three components: i) dual-axis laser scanning unit, ii) a separation unit of fluorescence and Raman signal for detection of F-SERS dots at the same time, iii) light detection unit with a photodiode for fluorescence signal and a spectrometer equipped with a CCD detector for SERS signal.

i) The dual-axis laser scanning unit was composed of two oscillating mirrors. Each mirror was oscillating for horizontal line scanning at the rate of 4-kHz, orthogonally, to allow real-time scan (12 frames/s). Thus, excitation laser was scanned the surface of optical fiber bundle and injected in each fiber of bundle. The laser sequentially injected in each fiber illuminated the sample, and the signals were collected by the same fiber. The collected signals involving fluorescence and Raman signal were separated by separation unit. ii) The separation unit was composed of two kinds of optical filters: dichroic filter and long-pass filter. The dichroic filter was allowed to transmit above 590 nm, and long-pass filter reflected under 532 nm. When the sample was illuminated, collected signal contained the fluorescence and Raman signal involving Rayleigh scattering, intrinsic Raman scattering of optical fiber bundle, and SERS signal. In order to detect the fluorescence and Raman signal simultaneously, the collected signal was separated by two optical filters. The

fluorescence signal, above 590 nm, passed through the dichroic filter to photodiode. Meanwhile, the Raman signal involving the Rayleigh scattering, intrinsic Raman scattering of optical fiber, and SERS signal, under 590 nm, was reflected by dichroic filter. After that, the Rayleigh scattering was rejected by the long pass filter to detect SERS signal. iii) The Raman scattering signals were detected by a spectrometer equipped with a detector CCD. The spectrometer was equipped with two diffraction gratings: 300 grooves/mm and 1800 grooves/mm.

An optical fiber bundle could be changed to another commercialized optical fiber bundle depending on the purpose. In this study, we used UltraMini-O (Mauna Kea Technologies, France) consisted of one hundred thousand of 2 μm sized optical fibers, and the diameter of this bundle was 4.2 mm. A lens was attached at the end of the optical fiber bundle for confocal detection. In this optical fiber bundle, the working distance was 60 μm and the field of view was 240 μm.

3. Results and Discussion

3.1 Design of real-time fluorescence-Raman endomicroscopic imaging system (FREIS)

The important issues of *in vivo* multiplex bio-imaging are ability to simultaneously detect multiple targets and penetrate superficial tissues. In this regard, real-time FREIS using the F-SERS dots with optical fiber bundle was designed to simultaneously detect fluorescence and Raman signal with real-time, in order to take the advantages of intense signal of fluorescence and multiplex capacity of Raman scattering; the fluorescence signal was utilized to imaging for fast tracking the targeted fluorescence-SERS probes (F-SERS dots), and the SERS signal was utilized to identify the kinds of F-SERS dots (see Figure 1). Further, FREIS has a significant advantage of non-limit of penetration depth because it was design to detect with optical fiber bundle, which could access to the proximal surface of the tissue. For these purposes, FREIS was designed to consist of three components (see Figure 2a): i) The dual-axis laser scanning unit, ii) the separation unit of fluorescence and Raman signal for detection of F-SERS dots at the same time, iii) light detection unit with a photodiode for fluorescence signal and a spectrometer equipped with a CCD detector for SERS signal.

Above all, for simultaneous detection of the fluorescence and Raman signal with real-time, the spectral range of fluorescence and Raman signal was designed to separate each other: fluorescence detection at above 2000 cm^{-1} and Raman detection

at under 2000 cm^{-1} (see Figure 2b). Further, as shown in Figure 3a and 3b, the optical beam paths of the fluorescence and Raman signal were modified in order to be independently detected by each detector such as the photo-diode for fluorescence signal and the spectrometer for Raman signal; through this modification of optical path, FREIS was allowed to simultaneously detect the fluorescence and Raman signal with real-time.

When a sample was measured by FREIS, the excitation laser illuminated to the sample via the dual-axis laser scanning unit which enable to real-time scanning (12 frames/s) using two oscillating mirrors. Due to two orthogonally oscillating mirrors at the rate of 4 kHz, the excitation laser was sequentially scanned and injected each fiber of optical fiber bundle composed of one hundred thousand of optical fiber. Meanwhile, the laser injected in each fiber illuminated the sample and collected signal by the same each fiber; namely, the excitation light and the collected signal have a same optical path. Thus, the collected signal of each fiber was synchronized with each position of fluorescence image. The collected signal was separated into the fluorescence signal and the Raman signal by dichroic filter. As shown in Figure 3a, the fluorescence signal was transmitted to photo-diode through the dichroic filter transmitting only above 2000 cm^{-1}. In this study, because the 532 nm laser line was used for excitation source, the rhodamine B isothiocyanate (RITC) emitting the fluorescence of approximately 590 nm (*ca.* 1850 $cm^{-1}$of Raman Shift) was chosen as fluorescence label. Even though the photo-diode only measured the intensity of

fluorescence, the collected fluorescence signal could construct the fluorescence image by synchronizing with position of individual optical fiber. As a result, FREIS was possible to provide the fluorescence image with real-time (12 images/s), which enable to track the targeted F-SERS dots. At the same time, the Raman signals were also detected by the spectrometer equipped with CCD detector to identify the kind of detected F-SERS dots (see Figure 3b). The Raman signals involving Rayleigh scattering, the intrinsic Raman scattering of optical fiber, and SERS signal were reflected by dichroic filter that reflect under 2000 cm^{-1}. After that, the Rayleigh scattering was rejected by long-pass filter, and only stokes-Raman signal was transmitted to spectrometer for Raman detection via the long-pass filter. However, when intrinsic Raman scattering of fiber and SERS signal were mixed, the SERS signal could not be distinguished because the intrinsic Raman scattering of optical fiber was very strong (see Figure 4). To circumvent this problem, spectral window with less background noises between 1250 and 2000 cm^{-1} was selected, and Raman reporter molecules were chosen to fit in the selected spectral window such as RITC, FITC, and 4-ABT. Each Raman reporter molecule has a characteristic strong band in SERS detectable range without spectral overlapping: 1356 and 1648 cm^{-1} of RITC, 1324 and 1633 cm^{-1} of FITC, and 1390 and 1436 cm^{-1} of 4-ABT. Therefore, FREIS can be applied to multiplexing detection of multiple targets at the same time.

FREIS used a fiber-coupled laser as excitation source in order to change more easily depending on the experimental purpose. In this study, the DPSS 532 nm fiber-

coupled laser was used; however, every fiber-coupled laser could be used for excitation source of FREIS. When another fiber-coupled laser is used, the two optical filters of separation unit will be changed to correspond with excitation wavelength. This feature provides the flexible selectivity of excitation wavelength.

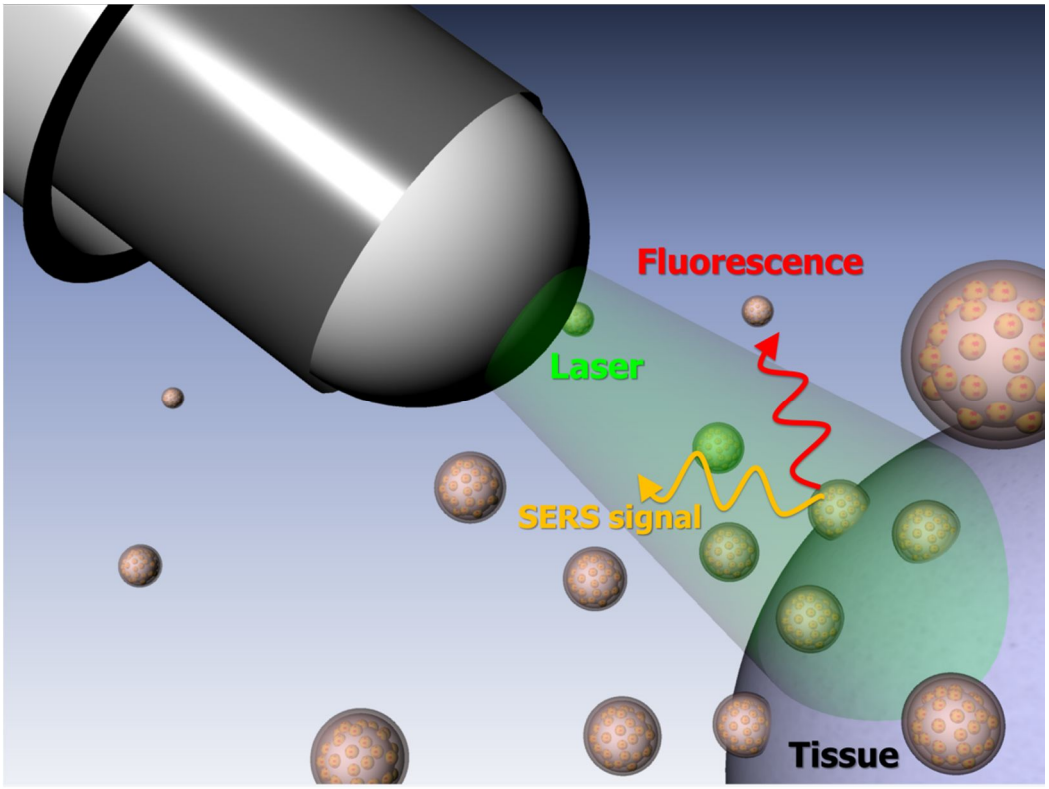

Figure 1. Illustration of detection of fluorescence-SERS probes using the fluorescence-Raman (dual modal) endomicroscopic imaging system (FREIS). The fluorescence image is utilized to quickly track position of the probe-targeted area, and SERS signal was utilized to identify the kind of probes.

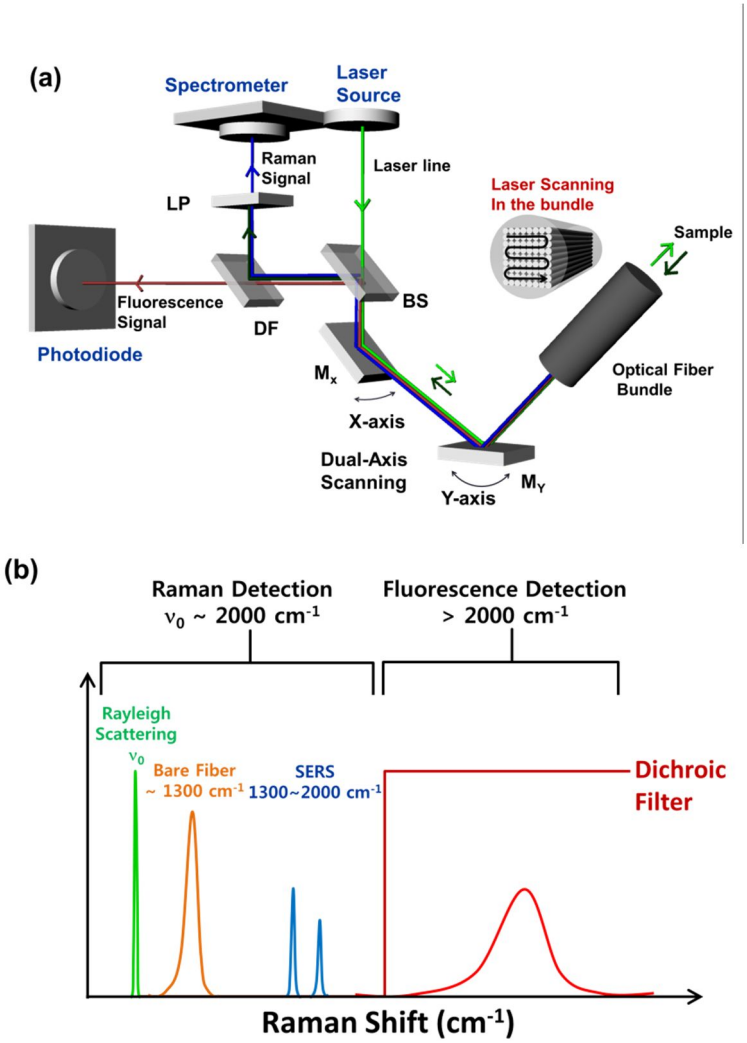

Figure 2. (a) Schematic diagram of the optical beam path of FREIS. BS: beam splitter, M_X: osilating mirror for X-axis, M_Y: oscillating mirror for Y-axis, DF: dichroic filter, and LP: long pass edge filter. (b) Illustration of the spectral design sectioning the ranges of collected signal from the sample. The collected signal contained the fluorescence signal and Raman signals involving Rayleigh scattering, intrinsic Raman scattering of optical fiber, and SERS signal.

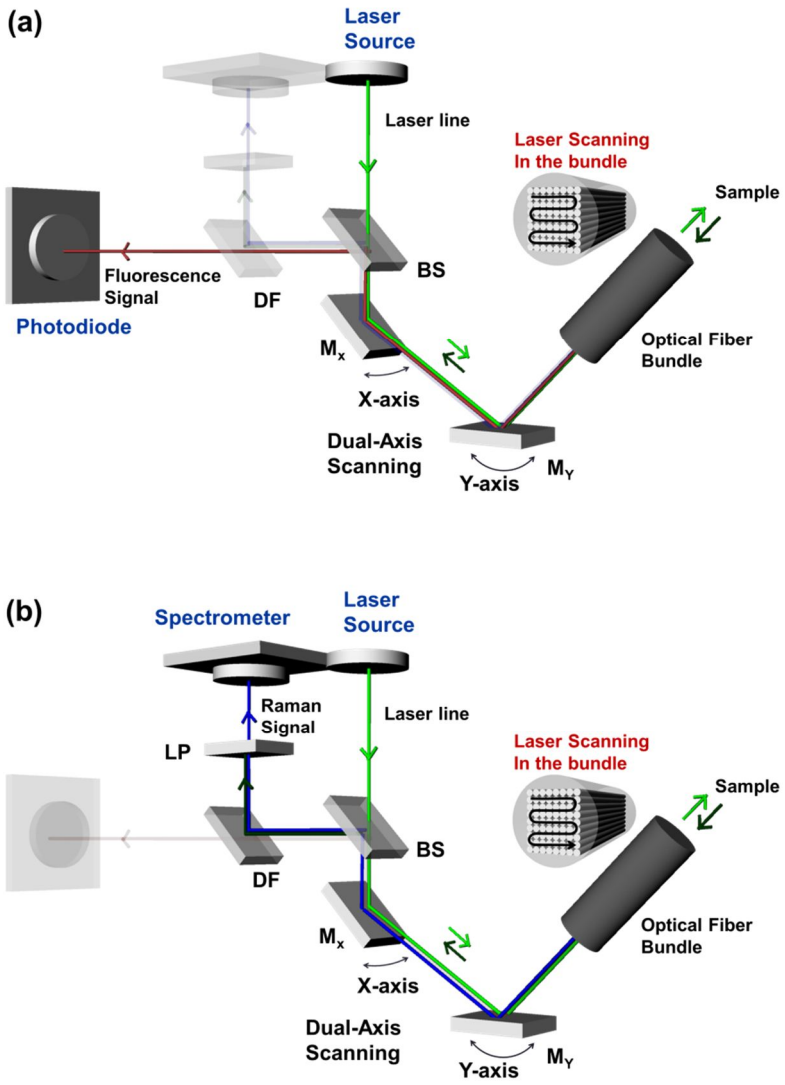

Figure 3. Schematic diagram of the optical beam path for fluorescence imaging (a), and Raman detecting (b). BS: beam splitter, M_X: osilating mirror for X-axis, M_Y: oscillating mirror for Y-axis, DF: dichroic filter, and LP : long pass edge filter.

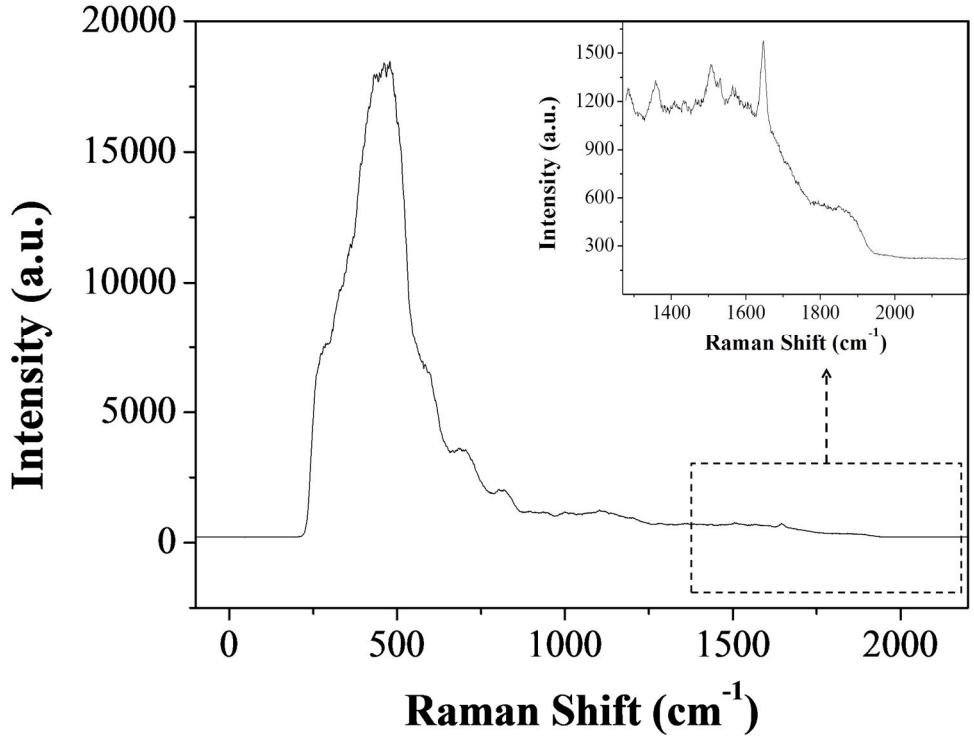

Figure 4. The Raman spectrum of optical fiber bundle with F_{RITC}-$SERS_{RITC}$ dots using FREIS. The inset is an enlarged spectrum showing less background noises; 1250 ~ 2200 cm^{-1}, which is the SERS detectable range.

3.2 Synthesis and characterization of the F-SERS dots

The silica nanoparticles (*ca.*120 nm) as a supporting material were synthesized (Figure 5a) by the Stöber method.[28] After surface of the silica nanoparticles (NPs) were modified with MPTS, silver nanoparticles were directly synthesized on the surface of thiol-functionalized silica NPs using the modified polyol method for preparing the silver nanoparticles embedded onto the silica NPs (Ag silica, Figure 5b). In this method, the octylamine was used as both a reducing agent and a stabilizer for the mild nucleation of silver NPs on the surface of silica NPs.[29] These Ag silica were labeled by three different kinds of Raman reporter molecules for multiplex detection: RITC, FITC, and 4-ABT; the Raman compounds were absorbed on the surface of silver NPs using the isothiocyanate and thiol functional groups (see Figure 5c). These Raman labeled Ag silica were coated by silica shell in order to prevent aggregation and fluorescence quenching (Figure 5d).[20] The silica shell coated SERS NPs were then treated with APS-organic dye (RITC)/TEOS under basic conditions to form F-SERS dots (Figure 5e). FREIS used above 2000 cm^{-1} of Raman shift as the fluorescence signal. In this study, the RITC, which emitted the fluorescence of approximately 590 nm (*ca.* 1850 cm^{-1} of Raman Shift), was chosen as fluorescence label because the 532 nm laser line was used for excitation source. As shown in Figure 6a, the synthesized F_{RITC}-$SERS_{RITC}$ dots were observed by Transmission Electron Microscope (TEM, JEM1010, JEOL); the size was *ca.* 240 nm.

To confirm that the F-SERS dots could emit fluorescence and SERS signal simultaneously, we measured three F-SERS dots (F_{RITC}-$SERS_{RITC}$ dots, F_{RITC}-$SERS_{FITC}$ dots, and F_{RITC}-$SERS_{4\text{-}ABT}$ dots) on the slide glass using standard micro-Raman spectrometer (LabRam 300, JY-Horiba). As shown in Figure 6b, the characteristic bands of each F-SERS dots were clearly observed and well-matched comparing with literature spectra.[30,31] Further, the fluorescence signal, RITC at *ca.* 580 nm, was observed from all kinds of F-SERS dots which were encapsulated by RITC-conjugated silica shell. These results confirmed that the F-SERS dots could be used as the dual modal probes with FREIS.

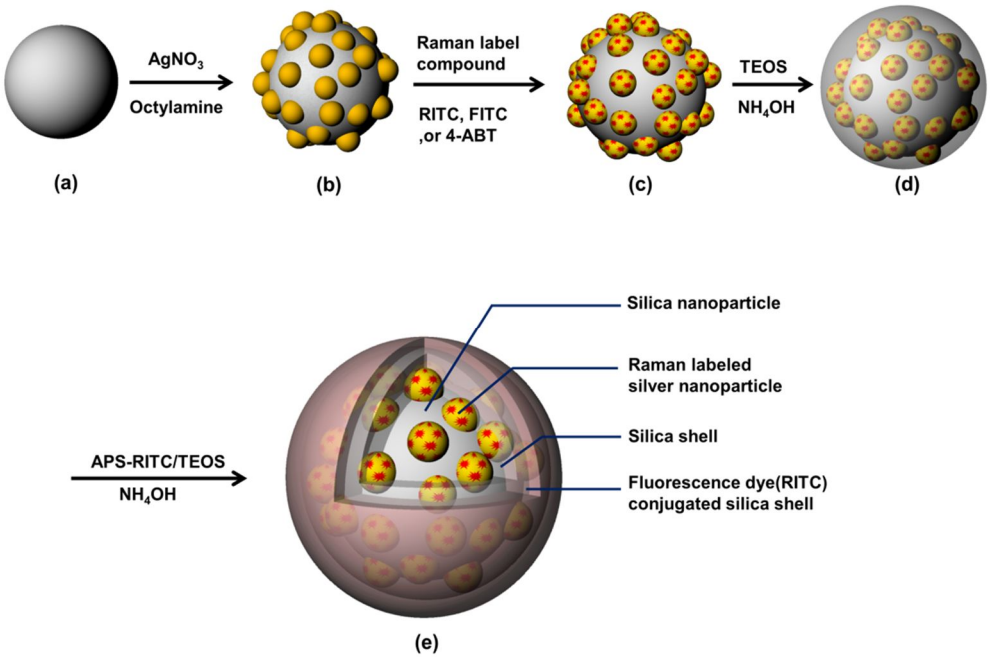

Figure 5. Schematic illustration of fabrication processes of fluorescence-SERS active nanoparticle (F-SERS dot). (a) Silica nanoparticle (NP), (b) silver-embedded silica NPs (Ag silica), (c) Raman-labeled Ag silica (SERS NPs) by RITC, FITC, or 4-ABT, respectively, (d) silica shell-coated SERS NPs, and (e) fluorescene dye (RITC) conjugated silica shell coated SERS NPs (F-SERS dot).

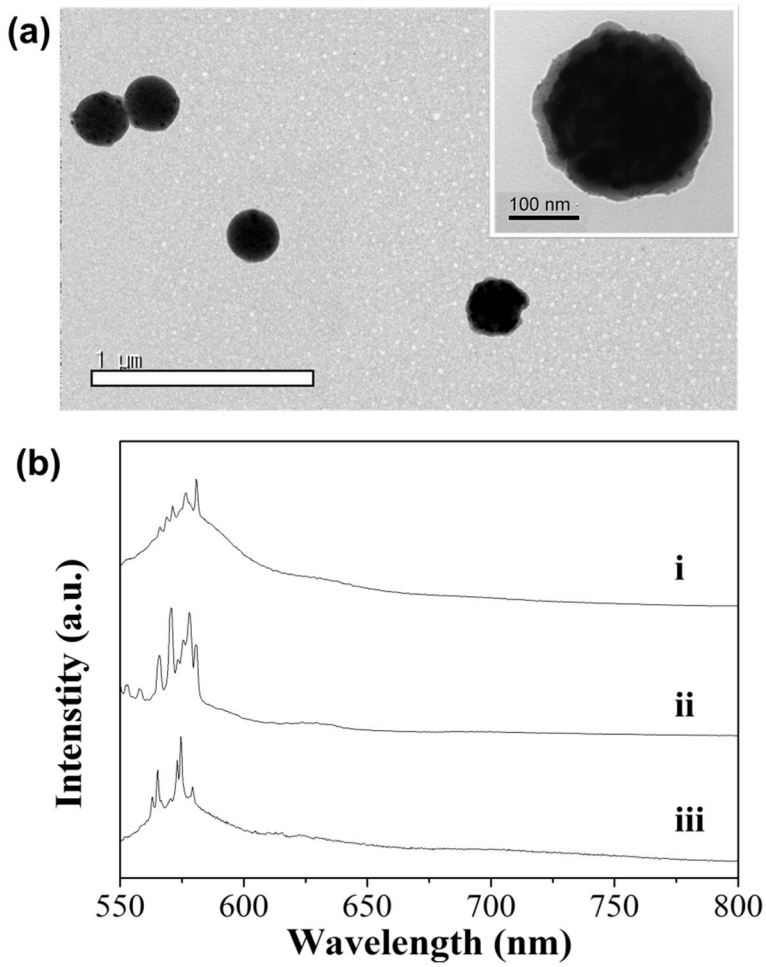

Figure 6. (a) Transmission electron microscopy (TEM) images of F_{RITC}-$SERS_{RITC}$ dots. The inset is a high magnified image of a F-SERS dot. (b) The Raman spectra of F-SERS dots with three different Raman compounds obtained with micro-Raman spectroscopy: i) F_{RITC}-$SERS_{RITC}$ dots, ii) F_{RITC}-$SERS_{FITC}$ dots, and iii) F_{RITC}-$SERS_{4\text{-}ABT}$ dots. All F-SERS dots were coated by RITC fluorescence dye conjugated silica shell. The Raman spectra were taken with 532 nm laser power of 0.31 mW, acquisition times of 10 s, and diffraction grating of 300 grooves/mm.

3.3 Evaluation of the measurement system

FREIS was compared with standard micro-Raman spectroscopy (LabRam 300, JY-Horiba) for evaluation of this system in terms of signal-to-noise ratio and resolution (see Figure 7). The Raman spectra of the F_{RITC}-$SERS_{RITC}$ dots were obtained by FREIS and the standard micro-Raman spectroscopy. The comparison of these two Raman spectra shows that FREIS has same overall performance between the standard spectroscopy in regards of signal-to-noise ratio and resolution.

FREIS was designed to detect fluorescence and Raman signal simultaneously. In order to confirm the simultaneous detecting ability, three different kinds of F_{RITC}-SERS dots: RITC, FITC, and 4-ABT, were measured on the slide glass. As shown in Figure 8, the fluorescence images and SERS spectra were taken by FREIS at the same point; these F-SERS dots were clearly distinguished from background in fluorescence images, and the characteristic bands of each compound were also observed in SERS spectra. Furthermore, the mixture of three different F-SERS dots was measured for multiplex detection. The Raman spectrum of the mixture shows that the specific bands of each labeled Raman compound were clearly distinguished: 1356 and 1648 cm^{-1} of RITC, 1324 and 1633 cm^{-1} of FITC, and 1390 and 1436 cm^{-1} of 4-ABT (see Figure 8b). These results indicated that this system could be utilized for multiplex detection using these F-SERS dots.

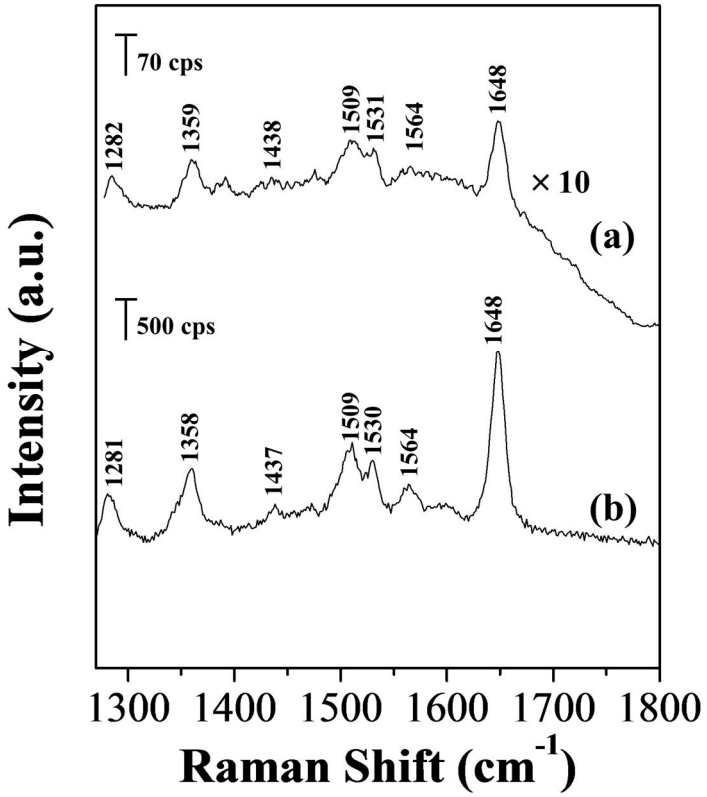

Figure 7. Raman spectra of F_{RITC}-$SERS_{RITC}$ dots on the slide glass using FREIS (a) and a standard micro-Raman spectroscopy (b) in order to compare in respect of signal-to-noise ratio and resolution. The Raman spectrum was taken with a laser power of 1.0 mW and acquisition time of 10 s using the multiplex imaging system; the Raman spectrum was taken with a laser power of 4.3 mW and acquisition time of 1 s using micro-Raman spectroscopy (LabRam 300, JY-Horiba). In order to compare to spectra, the base-line offset was given to all spectra.

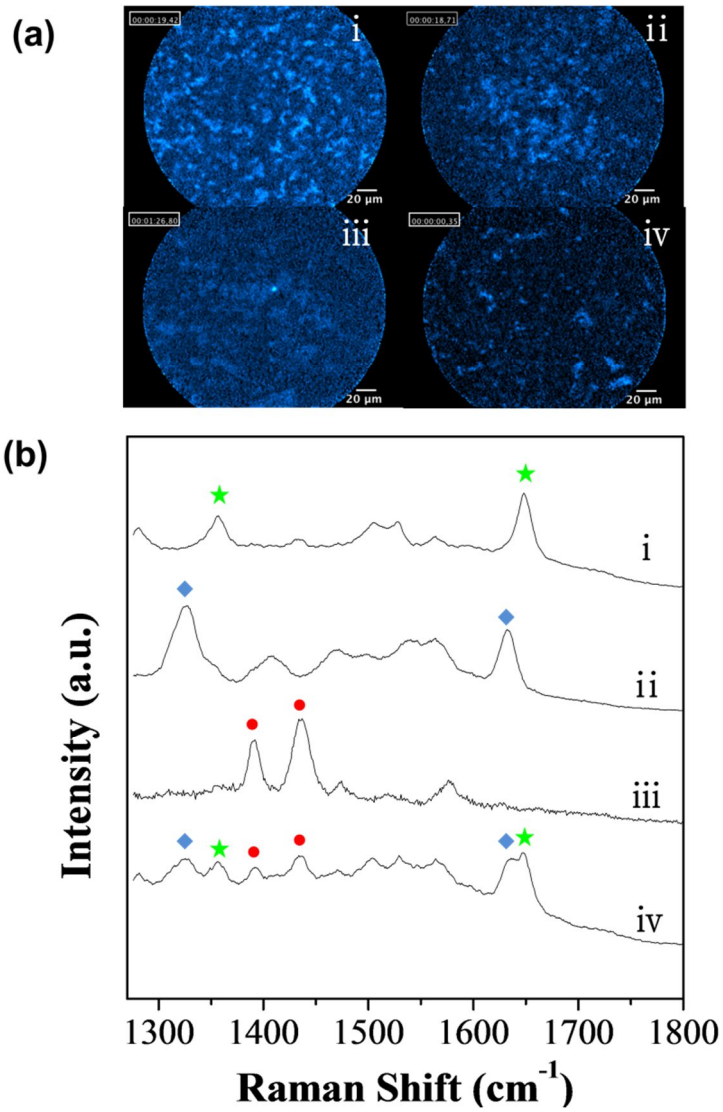

Figure 8. Fluorescene images (a) and Raman spectra (b) of three different F-SERS dots and their mixture: i) F_{RITC}-$SERS_{RITC}$ dots, ii) F_{RITC}-$SERS_{FITC}$ dots, and iii) F_{RITC}-$SERS_{4\text{-}ABT}$ dots, and iv) a mixture of the three. All images and spectra were obtained by FREIS on the slide glass. The SERS spectra were integrated for 10 s. In order to compare to spectra, the base-line offset was given to all spectra.

3.4 Determination of limits of detection

As shown in Figure 9, various concentrations of F_{RITC}-$SERS_{RITC}$ dots were measured by FREIS for determination of the sensitivity of this system. The different concentrations of F_{RITC}-$SERS_{RITC}$ dots were prepared from 2.5 to 0.02 mg/mL. The fluorescence image and the SERS spectra were obtained from each concentration of F_{RITC}-$SERS_{RITC}$ dots in the conical tube. The fluorescence images show that the number of these probes decreases with decreasing of concentration. At 0.02 mg/mL, several F_{RITC}-$SERS_{RITC}$ dots were even detected. In SERS spectra, the SERS intensity of characteristic band of RITC at 1649 cm^{-1} also decreases as concentration of these probes decreases; it was represented to SERS intensity graph (see inset in Figure 9b), which had linear relationship between the intensity and the concentration. Based on these results, we confirmed that the limit of detectable concentration was approximately 0.16 mg/mL for F_{RITC}-$SERS_{RITC}$ dots. These results implied that weak signals of fluorescence and SERS signal, which were emitted from a small number of F_{RITC}-$SERS_{RITC}$ dots, could be detected by this system simultaneously.

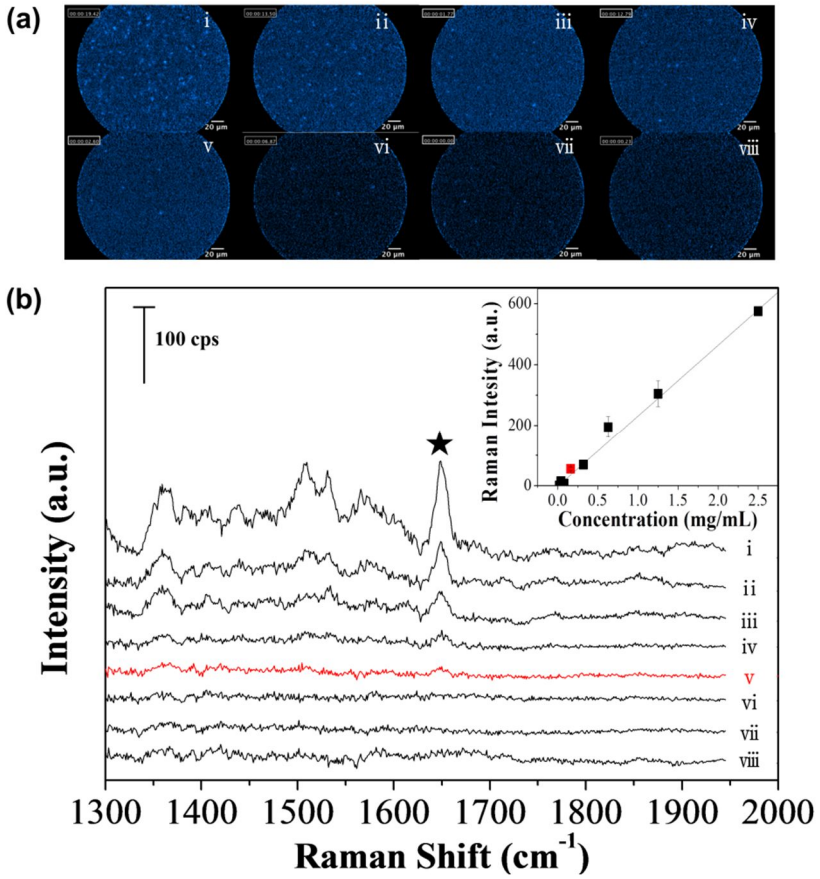

Figure 9. Evaluation of detetection limit of fluorescence and SERS signal using FREIS. (a) Fluorescence images of different concenctrations of F_{RITC}-$SERS_{RITC}$ dots: i) 2.5, ii) 1.25, iii) 0.63, iv) 0.32, v) 0.16, vi) 0.08, vii) 0.04, and viii) 0.02 mg/mL. (b) SERS specta of different concenctrations of F_{RITC}-$SERS_{RITC}$ dots. The inset in (b) is SERS intensity graph of the characteristic band of RITC at 1649 cm^{-1}(★). The concentration of detection limit was approximately 0.16 mg/mL, which is marked with red color(v). In order to compare to spectra, the base-line offset was given to all spectra.

3.5 Detection of F-SERS dots on the surface of phantom tissue

To demonstrate *in vivo* and *in situ* multiplex detection, we investigated that three F-SERS dots (F_{RITC}-$SERS_{RITC}$ dots, F_{RITC}-$SERS_{FITC}$ dots, and F_{RITC}-$SERS_{4\text{-}ABT}$ dots) were measured by FREIS at the surface of phantom tissue. At first, various concentrations of F_{RITC}-$SERS_{RITC}$ dots from 10 to 0.08 mg/mL were spread out to different regions on the surface of phantom tissue; after that, these regions were measured using this system respectively. As shown in Figure 10, the fluorescence images and SERS spectra were obtained at those regions. The fluorescence image of region, which was not treated by F_{RITC}-$SERS_{RITC}$ dots, could not detect any fluorescence signal; however, when F_{RITC}-$SERS_{RITC}$ dots were spread out, the probes image was clearly observed on the surface of phantom tissue (see Figure 10a). The SERS spectra were also supported that bright regions of fluorescence image were caused from fluorescence of F_{RITC}-$SERS_{RITC}$ dots because the SERS spectra show the specific bands of RITC (see Figure 10b). Next, the mixture of three different F-SERS dots (F_{RITC}-$SERS_{RITC}$ dots, F_{RITC}-$SERS_{FITC}$ dots, and F_{RITC}-$SERS_{4\text{-}ABT}$ dots) was spread out and measured by this system on the surface of phantom tissue for multiplex detection. As shown in Figure 9c and 9d, each F-SERS dots (F_{RITC}-$SERS_{RITC}$ dots, F_{RITC}-$SERS_{FITC}$ dots, and F_{RITC}-$SERS_{4\text{-}ABT}$ dots) could not be distinguished in the fluorescence image; on the other hand, the SERS signal was clearly separated in the SERS spectrum. These results indicated that FREIS could

track and identify targeted F-SERS dots on the surface of tissue simultaneously; further, it could be applied for *in vivo* multiplex bio-imaging.

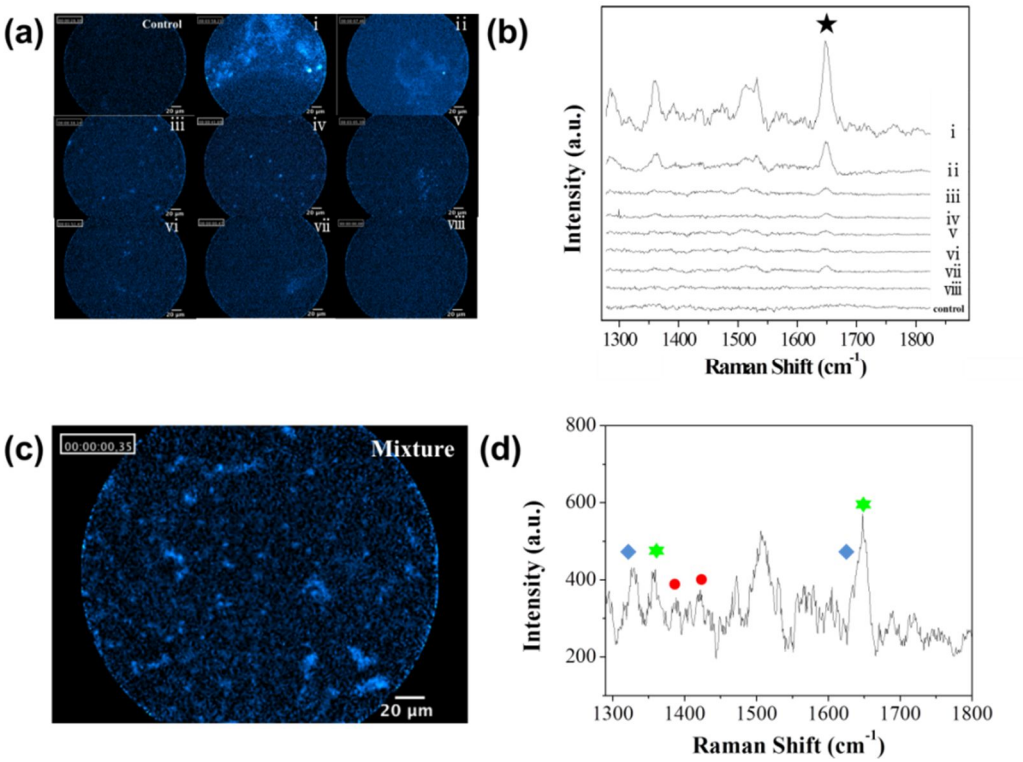

Figure 10. Detection of F_{RITC}-$SERS_{RITC}$ dots spread on the surface of phantom tissue using FREIS. Fluorescence images (a) and Raman spectra (b) of bare tissue and various concentration of F_{RITC}-$SERS_{RITC}$ dots, which were spread out on the surface of phantom tissue: i) 10, ii) 5, iii) 2.5, iv) 1.25, v) 0.63, vi) 0.32, vii) 0.16, and viii) 0.08 mg/mL. Fluorescence images (c) and Raman spectra (d) of a mixture of three different kinds of F-SERS dots Raman-labeled with RITC, FITC, and 4-ABT. The spectrum shows characteristic bands of each Raman compounds: 1356 and 1648 cm^{-1} of RITC(★), 1324 and 1633 cm^{-1} of FITC(◆), and 1390 and 1436 cm^{-1} of 4-ABT(●). In order to compare to spectra, the base-line offset was given to all spectra.

4. Conclusion

In summary, sensitive real-time fluorescence-Raman (dual modal) endo-microscopic imaging system (FREIS) with the fluorescence-SERS active nano-probes (F-SERS dots) were developed for multiplexed diagnosis. FREIS was designed to detect the fluorescence and SERS signal simultaneously. For this purpose, FREIS was designed to consist of three components: i) dual-axis laser scanning unit, ii) separation unit of fluorescence and Raman signal, iii) light detection unit with a photodiode for fluorescence signal and a spectrometer equipped with a CCD detector for SERS signal. Due to these components, FREIS could provide the fluorescence image tracking the targeted probes with real-time (12 images/s) and detect the SERS signal for identifying the kinds of probes. Further, the three different kinds of F-SERS dots were synthesized for multiplex detection: F_{RITC}-$SERS_{RITC}$ dots, F_{RITC}-$SERS_{FITC}$ dots, and F_{RITC}-$SERS_{4\text{-}ABT}$ dots. FREIS and the F-SERS dots were evaluated for capability of simultaneous and multiplex detection on the glass and the phantom tissue. As a result, the fluorescence and SERS signal emitted from the F-SERS dots were well-separated by optical filter of separation unit, and the fluorescence images and Raman spectra were obtained at the same time; the mixture of three different kinds of F-SERS dots was clearly distinguished by SERS spectra. These results implies that the developed imaging method comprised of optical system and F-SERS probes can be applied to real-time *in vivo* multiplex bio-imaging utilizing advantages of fluorescence and Raman spectroscopy.

5. References

1. P. Fortina, L. J. Kricka, S. Surrey, P. Grodzinski, Trends Biotechnol., 23, 168, 2005.
2. X. Mixchalet, et al., Science, 307, 538, 2005.
3. KK. Jain, Med Princ Pract., 17, 89, 2008.
4. X. Qian, X. H. Peng, D. O. Ansari, Q. Y. Goen, G. Z. Chen, D. M. Shin, L. Yang, A. N. Young, M. D. Wang, S. Nie, Nat. Biotechnol., 26, 83, 2008.
5. K. K. Maiti, U. S. Dinish, C. Y. Fu, J. J. Lee, K. S. Soh, S. W. Yun, R. Bhuvaneswari, M. Olivo, Y. T. Chang, Biosensors and Bioelectronis, 26, 398, 2010.
6. G. V. Maltzahan, A. Cenrtone, J. h. Park, R. Ramanathan, M. J. Sailor, T. A. Hatton, S. N. Bhatia, Adv. Mater., 21, 3175, 2009.
7. C. L. Zavaleta, B. R. Smith, L. Walton, W. Doering, G. Davis, B. Shojaei, M. J. Natan, S. S Gambhir, PNAS, 32, 13511, 2009.
8. K. N. Yu, S. M. Lee, J. Y. Han, H. M. Park, M. A. Woo, M. S. Noh, S. K. Hwang, J. T. Kwon, H. Jin, Y. K. Kim, P. J. Hergenrother, D. H. Jeong, Y. S. Lee, M. H. Cho, Bioconjugate Chem., 18, 1155, 2007.
9. M. A. Woo, S. M. Lee, G. S. Kim, J. H. Baek, M. S. Noh, J. E Kim, S. J. Park, A. M. Tehrani, S. C. Park, Y. T. Seo, Y. K. Kim, Y. S. Lee, D. H. Jeong, M. H. Cho, Anal. Chem., 81, 1008, 2009.
10. J. Qian, L. Jiang, F. Cai, D. Wang, S. He, Biomaterials, 32, 1601, 2011.

11. N. Stone, K. Faulds, D. Graham, P. Matousek, Anal. Chem., 82, 3969, 2010.

12. A. Burns, H. Ow, U. Wiesner, Chem. Soc. Rev., 35, 1028, 2006.

13. M. Brachez, M. Moronne, P. Gin, S. Weiss, A. P. Alivisatos, Science, 281, 2013, 1998.

14. W. C. W. Chan, S. Nie, Science, 281, 2016, 1998.

15. A. M. Derfus, W. C. W. Chan, S. N. Bhatia, Nano Lett., 4, 11, 2004.

16. C. L. Zavaleta, K. B. Hartman, Z. Miao, M. l. James, P. Kempen, A. S. Thakor, C. H. Nielsen, R. Sinclair, Z. Cheng, S. S. Gambhir, Small, 7, 2232, 2011.

17. S. Schlücher, Chem. Phys. Chem., 10, 1344, 2009.

18. K. K. Maiti, U. S. Dinish, A. Samanta, M. V. Vendrell, K. S. Soh, S. J. Park, M. Oivo, Y. T. Chang, Nano Today, 7, 85, 2012.

19. A. Samanta, K. K. Maiti, K. S. Soh, X. Liao, M. Vendrell, U. S. Dinish, S. W. Yun, R. Bhuvaneswari, H. Kim, S. Rautela, J. H. Chung, M. Olivo, Y. T. Chang, Angew. Chem. Int. Ed., 50, 6089, 2011.

20. S. Y. Lee, H. A. Chon, S. Y. Yoon, E. K. Lee, S. Chang, D. W. Lim, J. B. Choo, Nanoscale, 4, 124, 2012.

21. A. M. Mohs, M. C. Mancini, S. Singhal, J. M. Provenzale, B. L. Jones, M. D. Wang, S. Nie, Anal. Chem. 82, 9085, 2010.

22. P. R. Stoddart, D. J. White, Anal. Bioanal. Chem., 394, 1761, 2009.

23. B. G. Saar, R. S. Johnston, C. W. Freudiger, X. S. Xie, E. J. Seibel, Optics Letters, 36, 2396, 2011.

24. K. H. Al-Gubory, Experimental Cell Research, 310, 474, 2005.

25. E. Laemmel, M. Genet, G. L. Goualher, A. Perchant, J. L. Gargasson, E. Vicaut, J. Vasc. Res., 41, 400, 2004.

26. O. R. Scepanovic, Z. Volyskaya, C. R. Kong, L. H. Galindo, R. R. Dasari, M. S. Feld, Rev. Sci. Instrum., 80, 043103, 2009.

27. M. S. Bergholt, W. Zheng, K. Lin, K. Y. Ho, M. The, K. G. Yeoh, J. B. Y. So, Z. Huang, Biosensor and Bioelectronics, 26, 4104, 2011.

28. W. Stöber, A. Fink, E. Bohn, J. Colloid Interface Sci., 26, 62, 1968.

29. H. Kang, T. Kang, S. Kim, J. H. Kim, B. H. Jun, J. Chae, J. Park, D. H. Jeong, Y. S. Lee, J. Nanosci. Nanotechnol., 11, 579, 2011.

30. D. M. Zhang, S. M. Ansar, K. K. Vangala, D. P. Jiang, J. Raman Spectrosc., 41, 952, 2010.

31. K. Kim, H. B. Lee, Y. M. Lee, K. S. Shin, Biosensors and Bioelectronics, 24, 1864, 2009.

국문 초록

최근, 살아있는 동물을 대상으로 질병의 조기진단이나 치료, 질병의 진행상황을 감시하기 위한 목적으로 형광 염료, 양자점, 단일 벽 탄소 나노튜브, 귀금속 나노구조체를 활용한 광학 다중 생체 이미징 기술이 발전되어 왔다. 특히, 금이나 은과 같은 귀금속 구조체의 표면에 분자가 흡착 되었을 때 라만 산란 신호가 크게 증가되는 표면 증강 라만 산란 현상을 활용한 귀금속 나노 표지자는 생체 내 다중 측정에서 필요한 민감도와 다중 측정 능력을 제공할 수 있다. 표면 증강 라만 산란 신호는 신호 폭이 좁으며, 여기 광의 선택이 자유롭고, 광 분해가 일어나지 않아 다수의 표지 신호를 한꺼번에 측정이 가능하기 때문에 다중 측정에 있어서 상당한 장점을 가지고 있다. 이러한 이유로 표면 증강 라만 산란 기술은 생체 내 다수의 표적물에 대한 다중 이미징 기술에 많이 활용되고 있다. 이뿐만 아니라 보다 효과적인 생체 내 다중 측정을 위해 형광, 라만, 양자점을 이용한 방법들의 장점을 융합하여 활용하는 기술도 많이 보고 된 바 있다.

본 연구에서는 형광의 강한 신호세기와 라만의 다중 측정 능력의 장점을 동시에 활용하기 위해, 형광과 SERS 신호를 동시에 방출 할 수 있는 형광-SERS 표지자를 사용하여 표적된 물질의 형광 신호와 SERS 신호를 동시에 측정이 가능한 실시간 형광-라만 내시경형 이미징 시스템을 고안하였다.

이를 위해, 실시간 형광-라만 내시경형 이미징 시스템은 1) 이중 축 레이져 탐색부, 2) 형광과 라만 신호의 분리부, 그리고 3) 광 신호 측정부로 구성하였다. 또한, 형광 신호로는 RITC, 라만 신호는 RITC, FITC, 4-ABT 를 가진 서로 다른 세 가지의 형광-라만 표지자 (F-SERS dots)을 합성하였다. 본 시스템을 활용하여 형광-라만 표지자 시료를 측정하였고, 시료로부터 받아들인 신호의 형광 신호와 SERS 신호를 성공적으로 분리하였다. 이 때, 형광 신호는 표적된 표지자의 위치를 파악할 수 있도록 형광 이미지를 구현하는 데 사용되며, SERS 신호는 F-SERS dots 의 종류를 구별하는데 사용된다. 본 시스템은 형광 이미지를 실시간으로 제공할 수 있기 때문에 (초당 12 장의 이미지), 실시간으로 표지자의 위치 추적이 가능하다. 또한 본 시스템은 광섬유 다발을 이용하여 측정하도록 고안되어 있으므로, 광섬유 기반의 내시경 기술이 가진 장점을 동일하게 갖고 있다. 반면, 광섬유 다발 고유의 강한 라만 신호가 라만 신호의 측정 가능 영역을 감소시키기도 한다. 이를 해결하기 위해, 광섬유 다발 고유의 라만 신호가 약한 영역을 SERS 신호가 측정 가능한 영역으로 선정하여, 해당 위치에서 강한 라만 신호를 갖는 라만 화합물을 선정하였다. 또한 본 시스템의 목적인 생체 내 다중 이미징 기능을 증명하기 위해 슬라이드 글라스와 유사 생체 조직 위에 분포되어있는 F-SERS dots 을 본 시스템을 이용하여 측정하였으며, 형광 이미지와 SERS 스펙트럼을 동시에 실시간으로 얻을 수 있었다. 본 실험 결과를 통해 본 연구에서 개발한 실시간 형광-라만

내시경형 이미징 시스템은 형광의 강한 신호세기와 라만의 다중 측정 능력의 장점을 동시에 활용하여 생체 내 다중 진단 이미징 기술에 활용이 가능할 것이라 판단된다.

주요어 : 형광, 표면 증강 라만 산란 (SERS), 실시간 다중 측정 생체 이미징, 실시간 형광-라만 내시경형 이미징 시스템 (FREIS)

학번 : 2010-21534